Abstract No: 6632

Simultaneous comparison of response to two different anti-PD1 drugs in the same patient using a human tumor histo-culture platform

Biswajit Das[1], Kowshik Jaganathan[1], Gowri Shankar K[1], C Jayaprakash[2], MS Ganesh[3], Amritha Prabha[3], Vijay Pillai[4], Syamkumar V[1], Chandan Bhowal[1], Rajashekar M[1], Oliyarasi M[1], Ritu Malhotra[1], Govindraj K[1], Nandini Pal Basak[1], Satish Sankaran[1,#,*]

[1]Farcast Biosciences Pvt Ltd, Bangalore, [2]DBR & SK Superspeciality Hospital, Tirupati, [3]Vydehi Multi Specialty Hospital, Bangalore, and [4]Mazumdar Shaw Medical Centre, Bangalore, India

#,* Presenting and corresponding author

Introduction

Based on preclinical and clinical study data, anti-programmed cell death protein 1 (PD-1) drugs Pembrolizumab (P), and Nivolumab (N) have been considered equivalent in terms of response efficacy. Both the antibodies have IgG4 backbone but vary considerably in terms of the PD-1 epitopes they bind to. Given that there is almost no overlap between the PD-1 binding sites there is a definite possibility of nuanced drug-dependent differences in patient response to treatment. These differences would not be possible to discern unless the same patient with the same tumor microenvironment were evaluated with both drugs simultaneously. We attempted to address this question using the near native Farcast™ TruTumor histo-culture platform.

Table 1: Specifications of Nivolumab and Pembrolizumab

Parameter	Pembrolizumab	Nivolumab
Epitope	PD-1 CD loop.	PD-1 N-loop.
Affinity (K_d)	29 pM	3.06 pM
Cmax	65.7 µg/ml	132 µg/ml
Prescribed dose	2 mg/kg IV over 30 min every 3 weeks	3 mg/kg IV over 60 min every 2 weeks
Clearance	0.2 L/d	0.2 L/d
Terminal half-life	26 days	26.7 days

*REF:Tan, S., et al., An unexpected N-terminal loop in PD-1 dominates binding by nivolumab. Nature communications, 2017. **8** (1): p. 1-10.*

Methods

Histo-Culture workflow: The tumor sample and matched blood was collected from consented patients. These were transported to lab at 4ºC and processed to generate explants that were distributed into arms. These arms were treated in culture with P (Cmax, Cmax/2, Cmax/4) or N (Cmax) for 72 hours. Supernatants were collected pre-drug addition and at every 24hrs interval and replaced with fresh media and drug.

Flow cytometry analysis: Tumor explants were dissociated post culture into single cells. Cells were stained with Live/Dead dye, and an antibody cocktail against immune cell lineage and activation markers. Data was acquired using BD LSR Fortessa Flow cytometer with appropriate compensation controls and was analyzed using FlowJo software.

Cytokine Analysis: The cultured supernatants collected at T_0, T_{24}, T_{48}, T_{72} were tested for the presence of cytokines namely IL10, IFN-g, TNF-a, Perforin, and Granzyme, using Luminex MagPix platform. Data was analyzed using MILLIPLEX™ Analyst software.

H&E & IHC: H&E staining was performed with 4µm sections obtained from the FFPE block using Leica automated multi-stainer system. CD8 and cleaved Caspase-3 IHC was performed with 4µm sections obtained from the FFPE block using Ventana IHC automated staining system. Scoring was performed by certified pathologists. From H&E-stained slides tumor content, immune content and infiltrating immune cells (% immune cell proximal to tumor nest) were evaluated. Cleaved Caspase-3 staining was evaluated in the tumor compartment.

NanoString Analysis: The RNA extracted arm-wise from the TMA (Tissue Micro Array) FFPE block was quantified using Tape Station and 50ng of RNA based on DV200 concentration was used for NanoString run with PanCancer IO360 panel. Data was normalized and analyzed using the nSolver™ Data Analysis software. Gene expression signatures (GES) were analyzed to evaluate response.

Statistical analysis: All data analysis and graphical representations were done using GraphPad Prism (Version 9). Wilcoxon matched-pairs signed rank t-test for paired data and Mann-Whitney t-test for unpaired data, was used to generate P-values. P value significance is represented as * (p<0.05) ** (p<0.01), *** (p<0.001), **** (p<0.0001). P-values are mentioned for near significant data (0.05-0.08) and omitted if p>0.08.

Farcast™ TruTumor Histoculture Platform

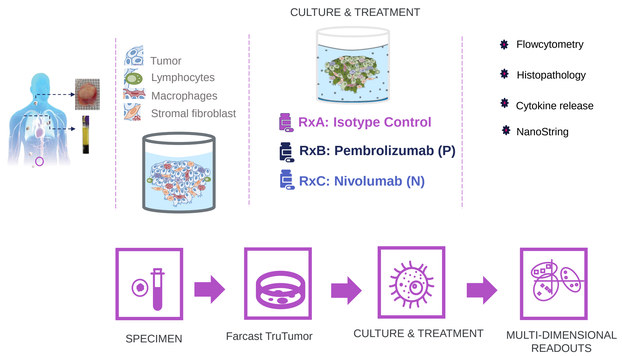

Fig 1: Schematic representation of experimental design and workflow during treatment.

Patient Demography

HNSCC (n=8)		
Parameters	**Category**	**Number (%)**
Age	<52	4 (50%)
	≥52	4 (50%)
Gender	Male	3 (37.5%)
	Female	5 (62.5%)
Grade	Grade 1	5 (62.5%)
	Grade 2	2 (25%)
	Grade 3	1 (12.5%)
	Sarcomatoid variant	1 (12.5%)
Stage	II	3 (37.5%)
	III	3 (37.5%)
	IV	1 (12.5%)
	IVA	1 (12.5%)
Recurrent/ Primary	Primary	8 (100%)
Neo adjuvant treatment given	No	0 (0%)
Tumor Site	Buccal Mucosa	5 (62.5%)
	Tongue	2 (25%)
	Lip	1 (12.5%)

Equivalent arms ensure reproducible response

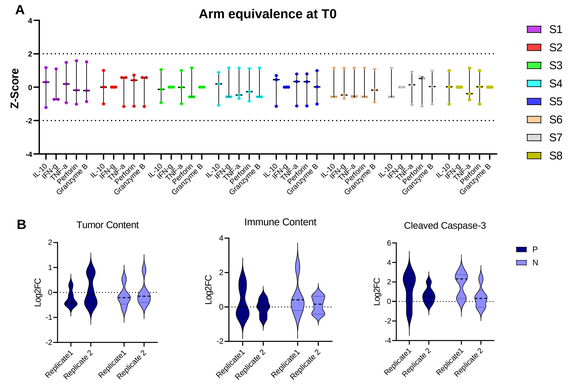

Fig 2: A. Box-whisker plot representing z-score of cytokine concentration (pg/ml) released before initiation of treatment (T0) for all samples. **B.** Violin plots representing tumor content, immune content and cleaved caspase-3 expression for duplicate treatment arms.

Pembrolizumab dose selection to obtain optimal response

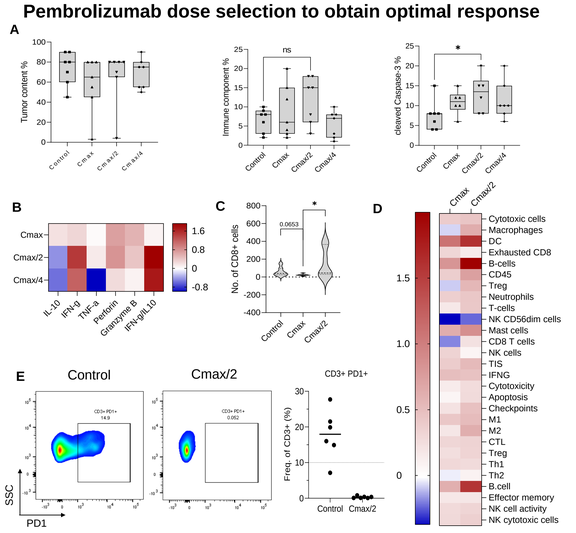

Fig 3: A. Percentage of tumor content, immune content and cleaved Caspase-3 plotted as a function of multiple doses (Cmax, Cmax/2 and Cmax/4) of Pembrolizumab. **B**. Heatmap of Log2FC of cytokines released during the treatment period. **C**. Total $CD8^+$ count on treatment with Cmax and Cmax/2. **D**. Heatmap of Log2FC of GES plotted upon treatment with Cmax and Cmax/2. E. Representation of flowcytometry data to evaluate receptor binding with Cmax/2 along with graphical representation of CD3+PD1+ masking (n=6).

Nuanced differences in response to Pembrolizumab and Nivolumab treatment across samples

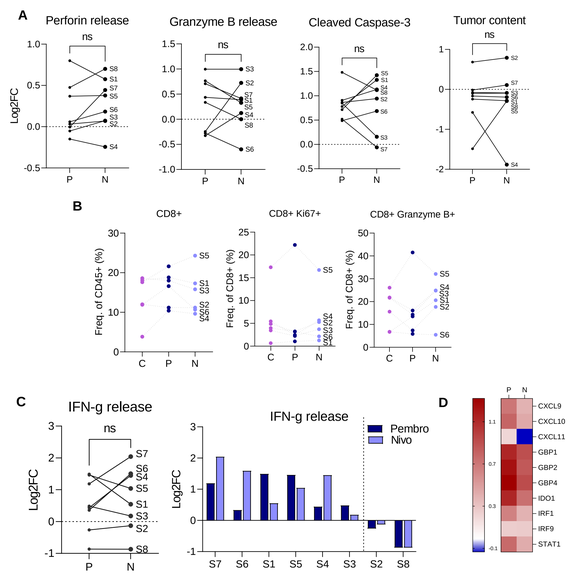

Fig 4: A. Log2FC of Perforin release, Granzyme B release, cleaved Caspase-3 expression, and tumor content for the cohort of 8 samples treated with P and N. **B.** Proportions of total and active CD8+ cells are plotted for control and treated arms. **C**. Log2FC of IFN-g released during treatment and the waterfall chart representation of the same where S2 and S8 are poor IFN-g responders to both treatment. **D**. Heatmap for Log2FC of IFN-g response genes upon treatment (n=3 samples showing IFN-g response).

Differential cytotoxic response to treatment with Pembrolizumab and Nivolumab across samples

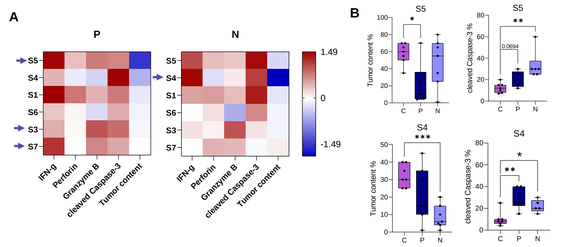

Fig 5: A. Heatmap is plotted for Log2FC wrt control of IFN-g release, Perforin release, Granzyme B release, cleaved Caspase-3 expression, and tumor content for both treatments (n=6 samples showing IFN-g response). Arrows indicate samples that comparatively responded better in that treatment arm. **B.** Graphical representation of tumor cytotoxicity for best responder with P treatment (S5) and N treatment (S4).

S3 exhibits better tumor cytotoxic response to Pembrolizumab treatment

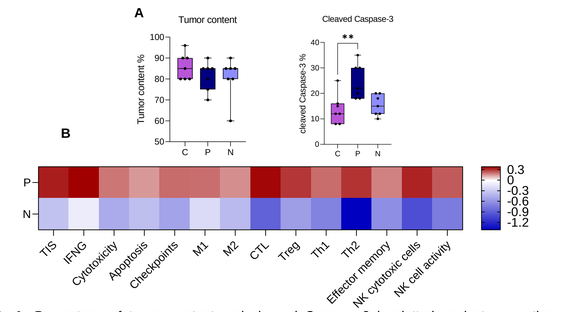

Fig 6: A. Percentage of tumor content and cleaved Caspase-3 is plotted against respective treatments. **B.** Heatmap for Log2FC of GES upon treatment.

Tumor cytotoxic response observed in S2 and S8 independent of IFN-g release

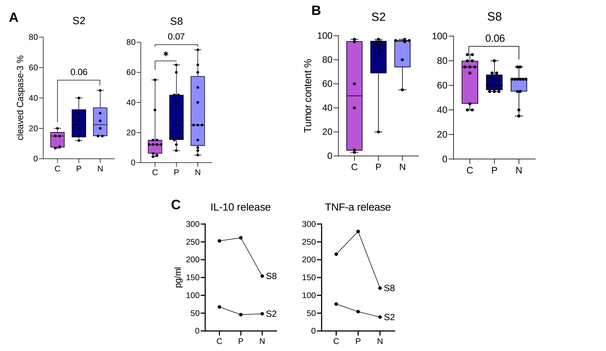

Fig 7: A. Tumor expression of cleaved Caspase-3 is plotted as a function of treatment for S2 and S8. **B**. Tumor content is plotted as a function of treatment for S2 and S8. **C**. Graphical representation of IL-10 and TNF-a released upon treatment.

S8 exhibited better tumor cytotoxicity response with Nivolumab treatment driven possibly by NK cells

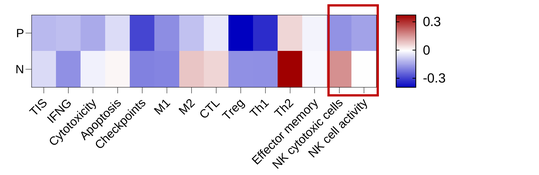

Fig 8: Heatmap for Log2FC of GES upon treatment wrt control. GES associated with NK cell are highlighted with red box.

Baseline analysis of S8 indicates an immunosuppressive TME in comparison to S7

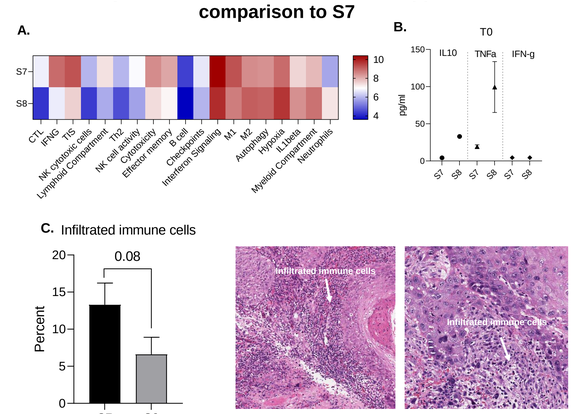

Fig 9: A. Heatmap for GES at baseline for S7 and S8. **B**. IL-10, TNF-a and IFN-g released before initiation of treatment are plotted for S7 and S8. **C**. Tumor infiltrated immune cells are plotted as a percentage of total immune cell for S7 and S8. Representative H&E image showing tumor infiltrated immune cell (white arrow) from S7 and S8.

Summary

Farcast™ TruTumor platform provides the unique opportunity to make personalized treatment choices that would provide the best response for that patient.